# Radio polarization measurement of meteor trail echoes during the 2012 Perseids

**Sylvain Ranvier, Michel Anciaux, Hervé Lamy, Johan De Keyser, Stijn Calders, and Emmanuel Gamby**

**Belgian Institute for Space Aeronomy (BIRA-IASB), 3, avenue Circulaire, B-1180 Brussels, Belgium**

sylvain.ranvier@aeronomie.be

We present radio polarization measurements of meteor trail echoes with a cross-polarized antenna of BRAMS, a network of radio receiving stations using forward scatter techniques to detect and characterize meteors.

## 1 Introduction

When using radio techniques to observe meteors, one way of gaining insights into the physical phenomena that produce the meteor echoes is by analyzing the radio polarization of meteor trail echoes (Billam and Browne, 1956; Sidorov et al., 1965; Cannon, 1986). For example, the time variation of the polarization of meteor echoes can, in principle, provide information about electron densities in the meteor trail as shown by Poulter and Baggaley (1977) and by Jones and Jones (1990). Furthermore, the physical phenomena that lead to specific signature of some echoes in the time-frequency domains, such as the multiple-branch echoes, the so-called "epsilons" (Steyaert, 2012), are still not fully understood. The analysis of the polarization of such echoes can be used to increase our knowledge in this field.

The paper is organized as follows. In Section 2, the current and future measurement set-ups are described. In Section 3, time variation of the polarization state for long and multiple-branch echoes is analyzed. In Section 4, conclusions are formulated.

*Figure 1* – Transmitting antenna in Dourbes, Belgium.

## 2 Measurement set-up

### 2.1 Current set-up

In this study, the forward scattering technique is used to analyze the meteors. The transmitter is the dedicated beacon of the BRAMS (Belgian RAdio Meteor Stations) network (Calders and Lamy, 2012) located in Dourbes, in the south-west of Belgium. The transmitting antenna is a crossed dipole with an 8 m × 8 m ground plane below, as shown in Figure 1. It emits towards the zenith a purely sinusoidal wave that is circularly polarized, at a frequency of 49.97 MHz and with a power of 150 W. The receiving station, which is located in Uccle, in the Brussels area (about 90 km away from the beacon), includes a crossed 3-element Yagi antenna (see Figure 2), and, therefore, allows measurements of all polarizations. The antenna is tilted 45° in elevation and 45° around its axis. In azimuth, the antenna is pointing in the direction of the beacon.

*Figure 2* – Receiving antenna in Uccle, Belgium.

Ideally, the main lobe of the antenna should be pointing 100 km above the beacon. But, due to the ground effect, when the antenna is tilted 45° in elevation and around its axis, as shown in Figure 2, the main lobe can be at about 30° in elevation, as can be seen in the simulated radiation pattern plotted in Figure 3.

From the simulated pattern shown in Figure 4, it is clear that the radiation pattern in azimuth is not symmetric. In addition, it has been noticed that, when the antenna is in that position, the radiation patterns in both azimuth and elevation are very sensitive to the ground properties (humidity, thickness, relative permittivity, etc.), which can change with time.

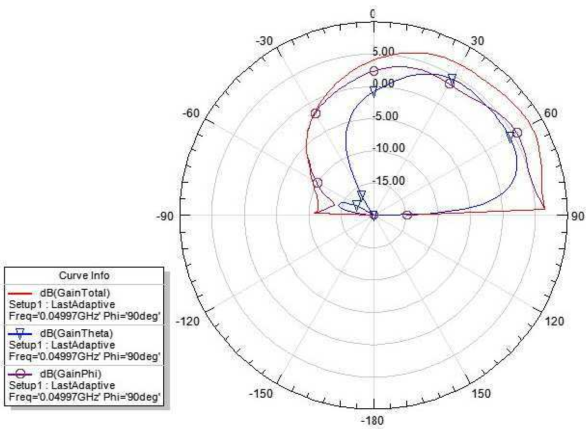


*Figure 3* – Simulated gain in elevation of a 3-element Yagi antenna tilted 45° in elevation and around its axis (half of the cross-polarized antenna). The azimuth is 45° from the antenna boom.

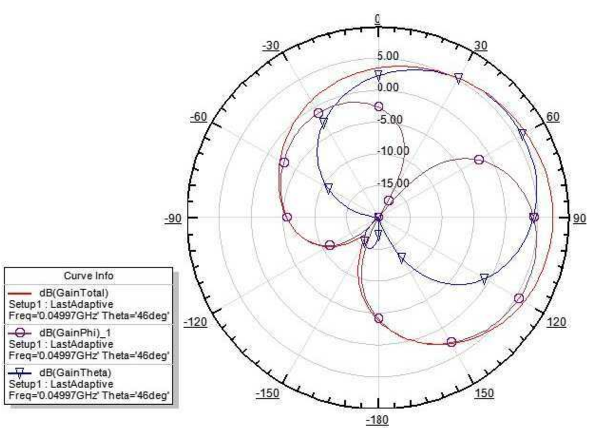


*Figure 4* – Simulated gain in azimuth of a 3-element Yagi antenna tilted 45° in elevation and around its axis (half of the cross-polarized antenna). The elevation is 46° from the ground.

As shown in Figure 5, the two receivers are synchronized with an external 10 MHz reference. The receivers are only frequency-coherent, not phase-coherent, and, therefore, have random phase when starting up. Signals from the two receivers and the one-pulse-per-second (PPS) signal from a GPS clock are sampled simultaneously at 11 025 Hz by an analog to digital converter (ADC) and then stored on a PC. We then carry out a FFT of the sampled signals to obtain spectrograms where meteor echoes can easily be distinguished from "spurious" echoes such as reflections on planes.

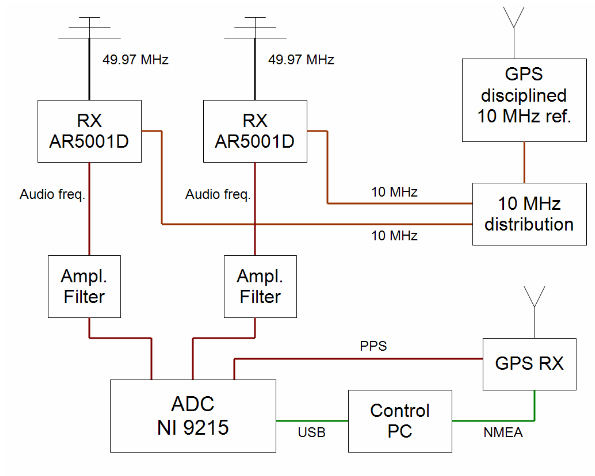


*Figure 5* – Current measurement set-up.

## 2.2 Future set-up

In order to ensure a proper phase and gain calibration of the set-up, we will insert a common reference signal a few KHz above the beacon frequency at the input of the receivers, as described in Figure 6. This will guarantee a continuous knowledge of the phase relation between the two receivers, even after power failure. By inserting the reference signal at the input of the receivers, the antenna and the cables will not be included into the calibration, but they are not likely to change significantly with time. This solution has been chosen, since, by inserting the reference signal at the antenna level, we would have made the calibration very sensitive to the immediate surroundings of the antenna. The radiation pattern (gain and phase) of the antenna will be measured only once.

To overcome the problems related to the radiation pattern of the receiving antenna mentioned in Section 2.1, the antenna will be tilted 90° in elevation (pointing to-

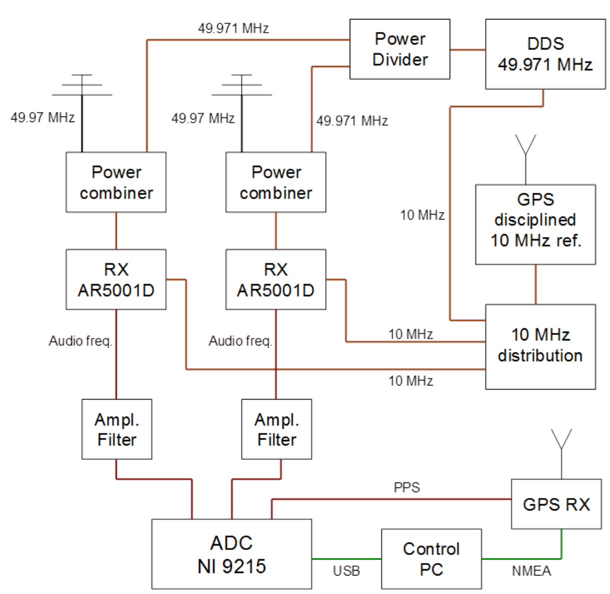


*Figure 6* – Future measurement set-up.

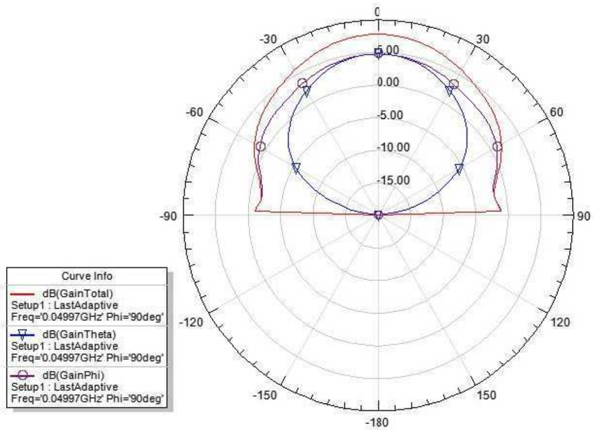


*Figure 7* – Simulated gain in elevation of a 3-element Yagi antenna pointing towards zenith (half of the cross-polarized antenna). The azimuth is 45° from the E-plane.

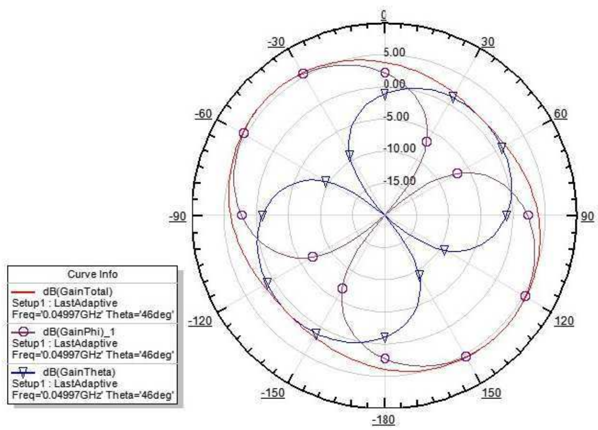


*Figure 8* – Simulated gain in azimuth of a 3-element Yagi antenna pointing towards zenith (half of the cross-polarized antenna). The elevation is 46° from the ground.

wards the zenith) instead of 45° currently. The corresponding simulated gains in elevation and azimuth are plotted in Figure 7 and Figure 8, respectively. In addition to the symmetry observed in both azimuth and elevation, the radiation pattern is much less sensitive to the properties of the ground.

## 3 Time variation of polarization state

### 3.1 Analysis method and limitations

Since the measurements during the 2012 Perseids were performed with the current measurement set-up (no reference signal, intermittent phase jumps, and problems with the radiation pattern of the receiving antenna), there are two limitations in the data interpretation. The first one is that we cannot determine the absolute polarization state of the incoming wave. Instead, we describe here the time variation of the four Stokes parameters, that are linked to the polarization state. The second limitation, due to the phase jumps, is that we cannot compare the Stokes parameters over a long period (several hours). Instead, we present here the time variation over the duration of the echoes (in the order of seconds or minutes). The four Stokes parameters are calculated using the following formulae:

$$I = |E_x|^2 + |E_y|^2;$$
$$Q = |E_x|^2 - |E_y|^2;$$
$$U = 2\Re(E_x E_y^*);$$
$$V = 2\Im(E_x E_y^*),$$

where $E_x$ and $E_y$ are the received signals from the dual polarized antenna (orthogonal polarizations). The degree of polarization, $I_\mathrm{p}$, is defined as follows:

$$I_\mathrm{p} = \frac{\sqrt{Q^2 + U^2 + V^2}}{I}.$$

### 3.2 Long echoes

In this Section, $I_\mathrm{p}$, $Q$, $U$, $V$, and $I/I_\mathrm{max}$, together with the associated spectrogram (see Figures 9 and 11), are plotted for two examples of long (overdense) echoes, which will be referred to as echo L1 and echo L2, and lasted 25 seconds and 45 seconds, respectively.

It is seen from Figure 10 that the polarization state of echo L1 is changing significantly, especially during the first 15 seconds (from second 80 to 95).

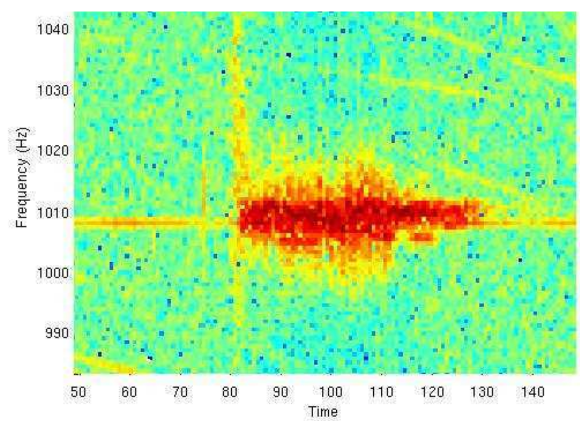


*Figure 9* – Spectrogram of echo L1.

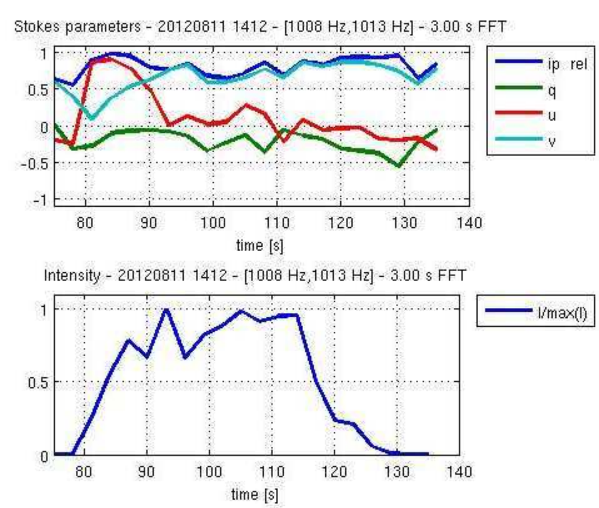


*Figure 10* – Parameters $I_\mathrm{p}$, $Q$, $U$, $V$, and $I/I_\mathrm{max}$ of echo L1.

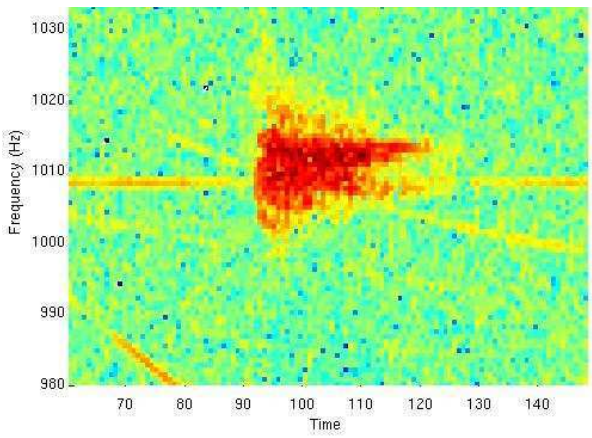


*Figure 11* – Spectrogram of echo L2.

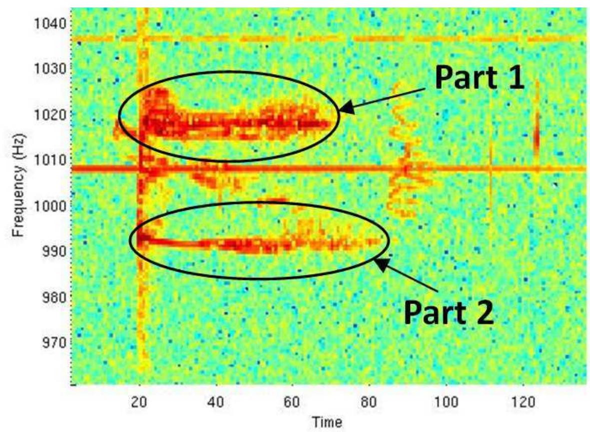


*Figure 13* – Spectrogram of echo MB1.

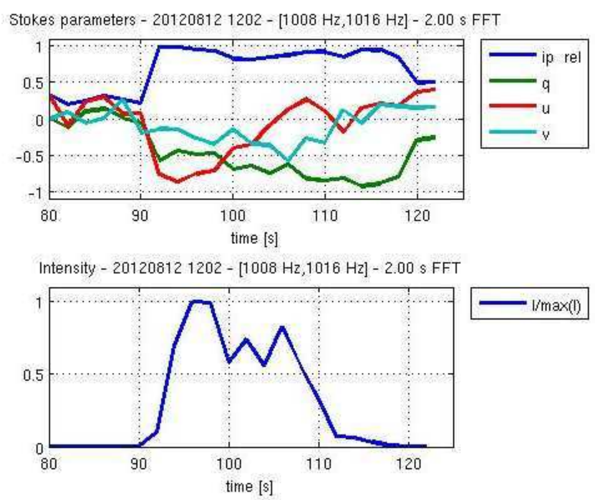


*Figure 12* – Parameters $I_{\mathrm{p}}$, $Q$, $U$, $V$, and $I/I_{\max}$ of echo L2.

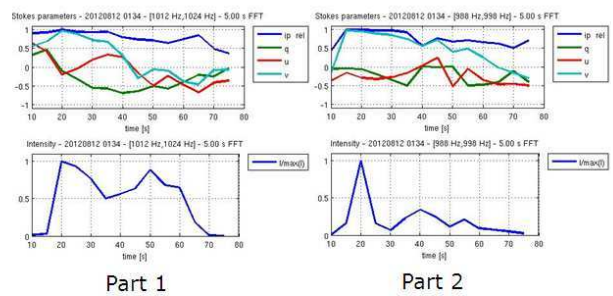


*Figure 14* – Parameters $I_{\mathrm{p}}$, $Q$, $U$, $V$, and $I/I_{\max}$ of echo MB1.

From Figure 12, one can notice that, similarly to echo L1, the polarization state of echo L2 is changing significantly with time. However, the changes now occur at the end of the echo (from second 105 to 120).

## 3.3 Multiple-branch echoes

In this Section, $I_{\mathrm{p}}$, $Q$, $U$, $V$, and $I/I_{\max}$, together with the associated spectrogram (see Figures 13 and 15) are plotted for two examples of (overdense) multiple-branch echoes, which will be referred to as echo MB1 and echo MB2. Each echo has been divided into two parts (separated in the frequency domain), which have been analyzed separately.

Similarly to the long echoes, the multiple-branch echoes exhibit time variations in their polarization states.

It is seen from Figure 14 that, although the Stokes parameters of the two branches follow globally the same trend with time, there are some noticeable differences between the polarization states of the two parts.

The Stokes parameters plotted in Figure 16 indicate that, in the same way as for echo MB1, the two branches of echo MB2 follow globally the same trend with the time, although there are some noticeable differences between the polarization states of the two parts.

## 4 Discussion

In this paper, the current and future measurement setups of the receiving station in Uccle are described. It is seen that an external reference signal is needed to calibrate the system, especially with respect to the phase, because of the nature of our receivers (only frequency-coherent). Nevertheless, this type of continuous calibration can be useful also with phase coherent receivers, since it mitigates any fluctuation in the reception chain. In addition, after thorough simulation of the radiation pattern of the cross-polarized antenna, it appears that the actual main lobe is not pointing exactly in the desired direction (100 km above the beacon) and, more importantly, the radiation pattern is not symmetrical and is very sensitive to the ground properties, which can vary with time (e.g., humidity). Because the 2012 Perseids were observed using the current measurement set-up, the data should be interpreted with caution. We do not present the absolute polarization state, but rather parameters that are linked to the polarization state. Still, it can be stated that, for the long echoes, the polarization state varies as a function of time. As for the multiple-branch echoes, the polarization state varies as well, and, although the two branches exhibit similar trend, there are some noticeable differences. In the fu-

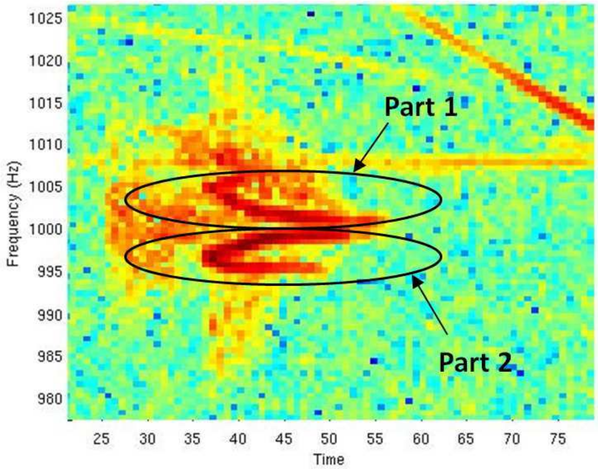


*Figure 15* – Spectrogram of echo MB2.

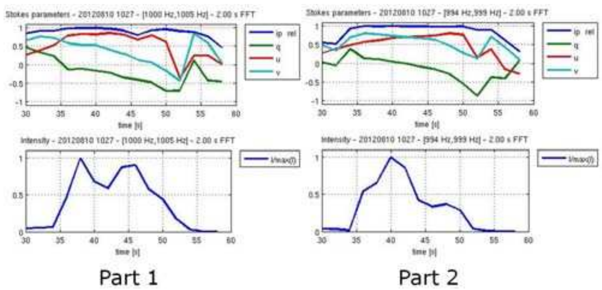


*Figure 16* – Parameters $I_{\mathrm{p}}$, $Q$, $U$, $V$, and $I/I_{\max}$ of echo MB2.

ture we will try to compare measurements with theoretical predictions, e.g., those by Sidorov et al. (1965).

## References


Billam E. R. and Browne I. C. (1956). “Characteristics of radio echoes from meteor trails IV: Polarization effects”. *Proc. Phys. Soc.*, **69**, 98–113.

Calders S. and Lamy H. (2012). “BRAMS: status and preliminary results”. In Gyssens M. and Roggemans P., editors, *Proceedings of the International Meteor Conference*, Sibiu, 15–18 September 2011, IMO, pages 73–76.

Cannon P. S. (1986). “Polarization rotation in meteor burst communication systems”. *Radio Science*, **21**, 501–510.

Jones W. and Jones J. (1990). “Oblique scattering of radio waves from meteor trains—Theory”. *Planetary and Space Science*, **38**, 55–66.

Poulter E. M. and Baggaley W. J. (1977). “Radiowave scattering from meteor ionization”. *Journal of Atmospheric and Terrestrial Physics*, **39**, 757–768.

Sidorov V. V., Pavlov A. F., and Fakhrutdinov R. Yu. (1965). “Phase techniques in the study of polarization phenomena associated with the reflection of radio waves from meteor trails”. *Izvestiya VUZ. Radiofizika*, **8**, 234–243.

Steyaert C. (2012). “Epsilons: we need more theories”. In Gyssens M. and Roggemans P., editors, *Proceedings of the International Meteor Conference*, Sibiu, 15–18 September 2011, IMO, pages 64–68.